EPJ Web of Conferences **137**, 07007 (2017) DOI: 10.1051/epjconf/201713707007
XIIth Quark Confinement & the Hadron Spectrum

Neutral meson production measurements with the ALICE at the LHC

Paraskevi Ganoti[1,a]
On behalf of the ALICE Collaboration

[1] *National and Kapodistrian University of Athens*

Abstract. Identified hadron spectra are considered to be sensitive to the transport properties of strongly interacting matter produced in high-energy nucleus-nucleus collisions. π^0 and η mesons in ALICE are identified via their two-photon decays by using calorimeters and the central tracking system. In the latter, photons are measured via their conversion to electron-positron pairs in the material of the inner ALICE barrel tracking detectors. The measured production spectra in pp, p−Pb and Pb−Pb collisions at mid−rapidity and over a wide p_T range will be presented in the available Large Hadron Collider (LHC) energies of Run I. The resulting nuclear modification factor R_{AA} at different centrality classes shows a clear pattern of strong suppression in the hot QCD medium with respect to pp collisions. Comparison of the ALICE results on neutral mesons with lower-energy experiments is also discussed.

1 Introduction

Light mesons such as π^0 and η provide a tool to test perturbative QCD (pQCD) with pp collisions, but also to study the properties of the QGP, which is created in ultra-relativistic heavy-ion collisions. These neutral mesons in pp collisions are produced from the fragmentation of partons created in hard processes during the early stages of the collision. Thus, the study of hadron production can provide constraints for the parton fragmentation functions (FF) and the parton distribution functions (PDF).

In heavy-ion collisions, the dense environment allows the observation of the modification of the FF or PDF via linear and non-linear recombination effects [1]. The Quark-Gluon Plasma formed in central heavy-ion collisions causes collisional energy loss and radiative parton energy loss induced by multiple scattering, that lead to modifications of parton fragmentation. The first observable of such phenomena, the yield suppression of inclusive hadrons in heavy-ion collisions compared to pp collisions, is arguably the most thoroughly studied quantity and provides a tool to extract the properties of the hot medium created in nucleus-nucleus collisions by comparing theoretical calculations with experimental measurements.

Measured neutral mesons give different information depending on their p_T range. At $p_T \lesssim 3-5$ GeV/c, they can give insight about collective effects via the modification of their p_T spectra. At the LHC energies, neutral mesons come mostly from gluon fragmentation. Due to the

[a] e-mail: pganoti@phys.uoa.gr

different color factor, gluons suffer a larger energy loss in the medium than quarks. This effect together with the different relative contribution of quarks and gluons to the π^0 and η production, lead to differences in the suppression pattern of the two particles [2, 3]. On the other hand, at $p_T \gtrsim 5$ GeV/c hadron production results from the hadronization of partons created in the initial hard scattering. These partons lose energy in the dense medium via radiation and collisions and this energy loss can be quantified via the measured neutral mesons spectra at high p_T.

2 Neutral meson reconstruction in the ALICE experiment

Neutral mesons are reconstructed in ALICE [4] by using four different detectors, the electromagnetic calorimeters PHOS [5] and EMCal [6] and the two tracking detectors, the ITS [7] (Inner Tracking System) and the TPC [8] (Time Projection Chamber).

In the calorimeters, the electron and photon reconstruction are made by measuring the electromagnetic showers produced by the incident particles.
PHOS is a high granularity and high energy resolution calorimeter installed at a radial distance of 4.6 m from the interaction point and is composed of lead-tungstate crystals, $PbWO_4$, of $2.2 \times 2.2 \times 18$ cm^3 dimensions and 0.89 cm radiation length. The pseudorapidity range covered is 0.26 units and the azimuthal coverage is 60°. The energy resolution is parametrized by the equation:

$$\frac{\sigma_E(GeV)}{E} = \frac{0.01}{E} \oplus \frac{0.04}{\sqrt{E}} \oplus 0.01. \tag{1}$$

The Electromagnetic Calorimeter (EMCal) is a Shashlik type Pb-scintillator sampling calorimeter built from alternating lead and scintillator segments of 1.44 mm and 1.76 mm thickness, respectively, together with longitudinal wavelength-shifting fibres for light collection. The cell (tower) size of the EMCal is approximately 0.014×0.014 rad in $\Delta\varphi \times \Delta\eta$ (6 cm) with a depth corresponding to 20.1 X_0. It is installed at a radial distance of 4.28 m from the interaction point and covers a pseudorapidity range of 1.4 units with 100° azimuthal coverage. The energy resolution of EMCal is described by the equation:

$$\frac{\sigma_E(GeV)}{E} = \frac{0.05}{E} \oplus \frac{0.11}{\sqrt{E}} \oplus 0.02. \tag{2}$$

The two tracking devices are used to reconstruct the tracks and the particle identification (to identify electrons and positrons) is made by measuring the energy loss of the tracks in those detectors. After identification, electrons and positrons are paired to reconstruct conversion photons. This is the Photon Conversion Method (PCM). The conversion point can be reconstructed with a z and φ resolution of 1.5 cm and 7 mrad, respectively. The photon conversion probability is rather small, $\sim$ 8.5%, but it is compensated by the wider acceptance of TPC: full azimuthal coverage and a pseudorapidity range of 1.8 units. The neutral mesons are reconstructed in the di-photon channel by using the invariant mass technique.

3 ALICE performance in the reconstruction of neutral mesons in Run I and Run II

ALICE has so far collected data from pp, Pb−Pb and p−Pb collisions at different energies. pp collisions have been recorded at $\sqrt{s}$ = 0.9, 2.76, 5.02, 7, 8 and 13 TeV, Pb−Pb collisions at $\sqrt{s_{\rm NN}}$ = 2.76 TeV and 5.02 TeV and p−Pb collisions at $\sqrt{s_{\rm NN}}$ = 5.02 TeV. In this section, the performance of

EMCal, PHOS and ITS/TPC (PCM method) is shown for some indicative energies and systems from Run I and Run II.

In Fig. 1, the invariant mass of two EMCal clusters in pp collisions at $\sqrt{s}$ = 7 TeV is shown for $16 < p_T^{\gamma\gamma} < 18$ GeV/c, where $p_T^{\gamma\gamma}$ is the photon pair transverse momentum. In Fig. 2, the two clusters invariant mass is shown in pp and Pb−Pb collisions at $\sqrt{s_{\rm NN}}$ = 2.76 TeV from the PHOS calorimeter and the PCM method. For the Pb−Pb collisions, two centrality classes are shown, 60−80% and the most central 0−10% in the p_T range $2.0 < p_T^{\gamma\gamma} < 2.5$ GeV/c for PHOS and $0.8 < p_T^{\gamma\gamma} < 1$ GeV/c for PCM. Figure 3 (left panel) shows the invariant mass distribution of two clusters from PHOS in pp collisions at $\sqrt{s}$ = 13 TeV (Run II data) in $4.5 < p_T^{\gamma\gamma} < 5$ GeV/c, while in the right panel the reconstructed π^0 peak from the PCM method in p−Pb collisions at $\sqrt{s_{\rm NN}}$ = 5.02 TeV and in the p_T range $1.20 < p_T^{\gamma\gamma} < 1.40$ GeV/c is presented.

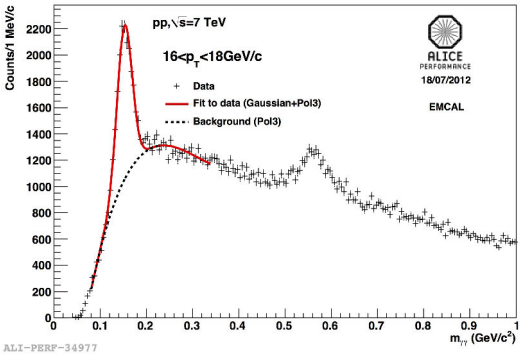

Figure 1. Invariant mass of photon pairs, reconstructed in the EMCal in pp collisions at $\sqrt{s}$ = 7 TeV.

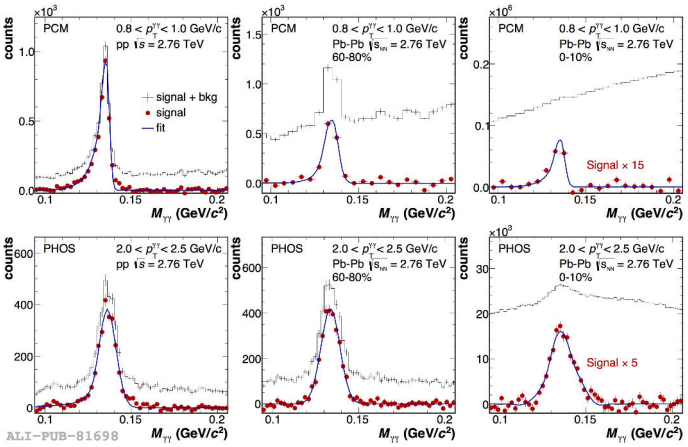

Figure 2. Invariant mass of photon pairs, reconstructed in the PHOS calorimeter and by the PCM method in pp and Pb−Pb collisions at $\sqrt{s_{\rm NN}}$ = 2.76 TeV [10].

4 π^0 and η spectra in pp collisions

ALICE has measured the p_T invariant differential production cross section of neutral mesons in pp collisions at all available centre-of-mass energies of Run I, 0.9, 2.76, 7 [9] (PHOS and PCM combined measurements) and 8 TeV (PHOS only preliminary result, [11]). In Fig. 4 (left panel), these π^0 spectra are presented fitted by a Tsallis function and compared to PYTHIA8 generator and to the next-to-leading order pQCD (NLO pQCD) calculations for two renormalization and factorization scales and

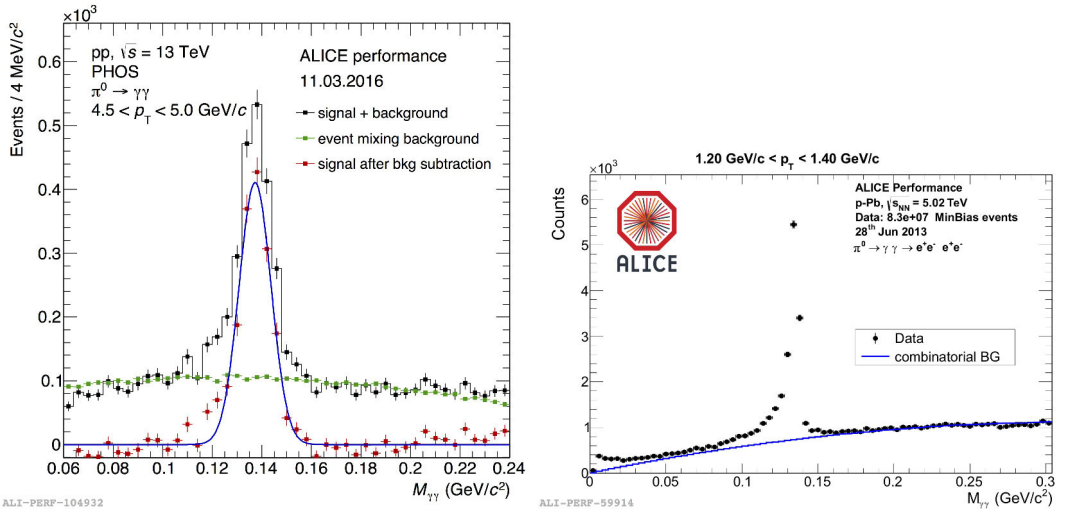

Figure 3. Left panel: Invariant mass of photon pairs, reconstructed in the PHOS calorimeter in pp collisions at $\sqrt{s}$ = 13 TeV. Right panel: Invariant mass of photon pairs, reconstructed by the PCM method in p−Pb collisions at $\sqrt{s_{\rm NN}}$ = 5.02 TeV

with the MSTW PDF and the DSS14 FF [12]. The π^0 spectra are better described by these calculations compared to previous ones [9], however, an increased discrepancy is observed between the data and the calculations with increasing p_T and centre-of-mass energy.

In Fig. 4 (right panel), the η spectra in pp collisions at $\sqrt{s}$ = 0.9, 2.76 and 7 TeV are shown. The spectra at $\sqrt{s}$ = 0.9 and 2.76 TeV are obtained from PCM only while the $\sqrt{s}$ = 7 TeV η spectrum is the combined result from PCM and PHOS. The spectra are compared to the NLO pQCD calculations with CTEQ6M5 PDF and the AES fragmentation function [9, 13]. This comparison reveals a bigger discrepancy compared to the π^0 case.

The η/π^0 ratio is presented in Fig. 5 for $\sqrt{s}$ = 2.76 and 7 TeV, respectively, and compared to the NLO pQCD calculations using CTEQ6M5 PDF for both particles and DSS FF for the π^0 and AES FF for the η [9]. Although this choice for the PDF and fragmentation functions does not reproduce the individual spectra, in the ratio their influence seems to be reduced. The ratio reaches above p_T = 4 GeV/c a constant value around four, compatible with the available world measurements.

5 π^0 and η spectra in Pb−Pb collisions at $\sqrt{s_{\rm NN}}$ = 2.76 TeV

The invariant neutral pion yields measured in pp and Pb−Pb collisions at $\sqrt{s_{\rm NN}}$ = 2.76 TeV in six centrality classes are shown in Fig. 6 [10]. This is the combined measurement from PCM and PHOS.

The modification of the hadron yields for different p_T intervals in heavy-ion (A-A) collisions with respect to pp collisions can be quantified with the nuclear modification factor:

$$R_{AA}(p_T) = \frac{\frac{d^2N_{AA}}{dp_T d\eta}}{< T_{AA} > \frac{d^2\sigma_{pp}}{dp_T d\eta}} \quad (3)$$

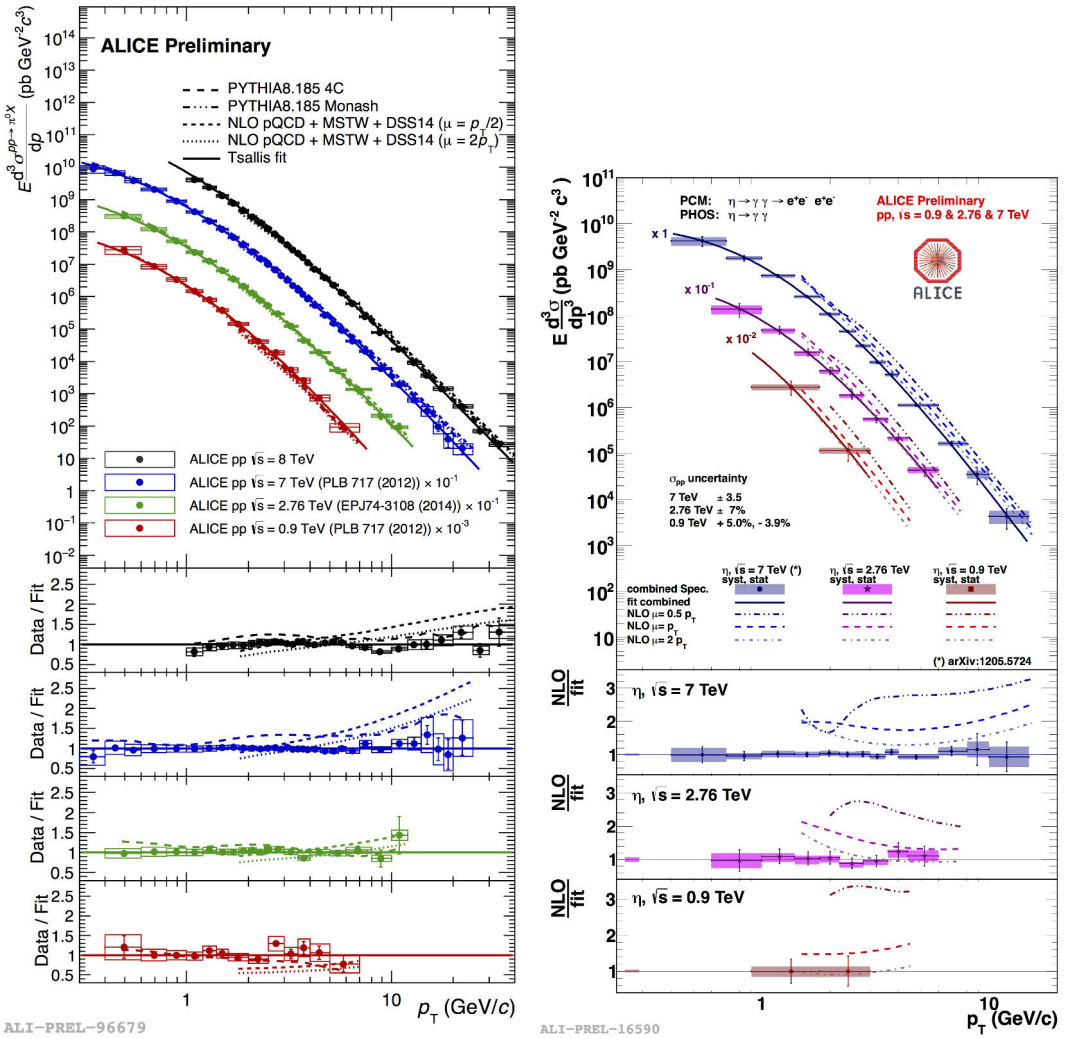

Figure 4. π^0 (left panel) and η (right panel) spectra in pp collisions at $\sqrt{s}$ = 0.9, 2.76, 7 TeV (and 8 TeV, π^0 only), compared to PYTHIA8 and NLO pQCD (MSTW + DSS for π^0 and CTEQ6M5 + AES for η) calculations.

where the nuclear overlap function $< T_{AA} >$ is related to the average number of inelastic nucleon-nucleon collisions as $< T_{AA} > = < N_{coll} > / \sigma^{pp}_{inel}$.

The combined R_{AA} from PCM and PHOS is shown in Fig. 7 (left panel), for three centrality classes: central (0-5%), semi-central (20-40%) and peripheral (60-80%). In all centrality classes the measured R_{AA} exhibits a maximum around $p_T \approx 1 - 2$ GeV/c. At high p_T, the observed suppression is attributed to an increasing energy loss in the medium with centrality. Agreement of R_{AA} between the neutral pions and the charged pions, kaons and protons is observed at high p_T [14].

The energy dependence of the R_{AA} has also been studied by comparing the ALICE results with those from previous [10] experiments (Fig. 7 right panel), WA98 at the SPS measurements in central

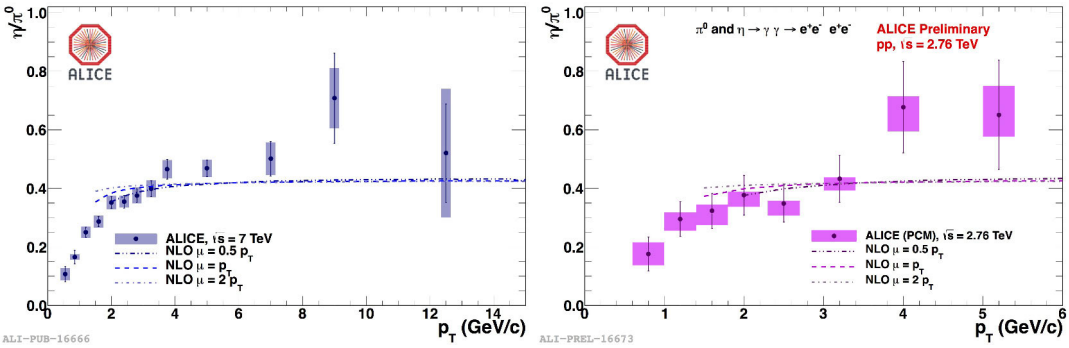

Figure 5. η/π^0 ratio in pp collisions at $\sqrt{s}$ = 7 TeV (left) [9] and $\sqrt{s}$ = 2.76 TeV (right), compared to NLO pQCD calculations.

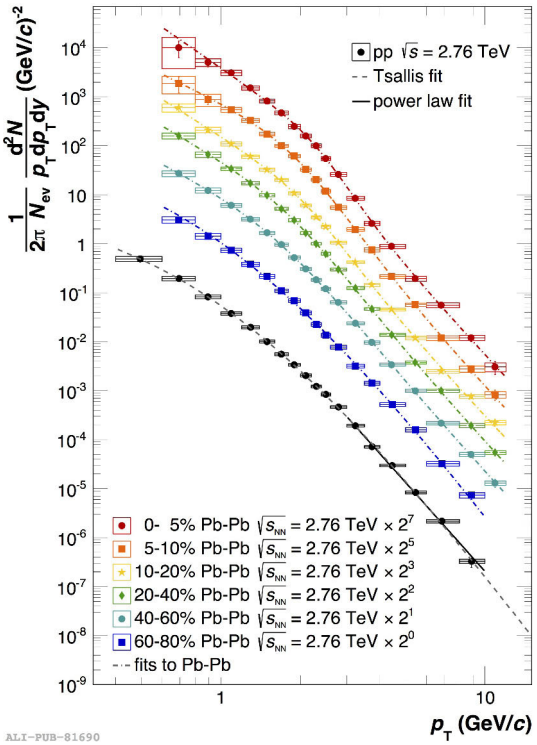

Figure 6. π^0 invariant yields in Pb−Pb collisions at $\sqrt{s_{\rm NN}}$ = 2.76 TeV from PCM and PHOS in six centrality classes [10], fitted by Tsallis and power law functions.

Pb−Pb events and PHENIX measurements in central Au−Au events at two energies. The decrease of the R_{AA} observed at the LHC energies compared to the lower centre-of-mass energies indicates that the higher initial energy densities created at larger $\sqrt{s_{\rm NN}}$ have a stronger influence in the R_{AA} compared to the harder initial parton p_T spectra. Considering the data for all shown energies one observes that the value of p_T with the maximum R_{AA} value appears to shift towards lower p_T with increasing $\sqrt{s_{\rm NN}}$.

The analysis of the 2011 Pb−Pb data collected by ALICE (10 times the integrated luminosity with respect to the results presented previously), allowed the extension of the p_T reach for π^0 up to

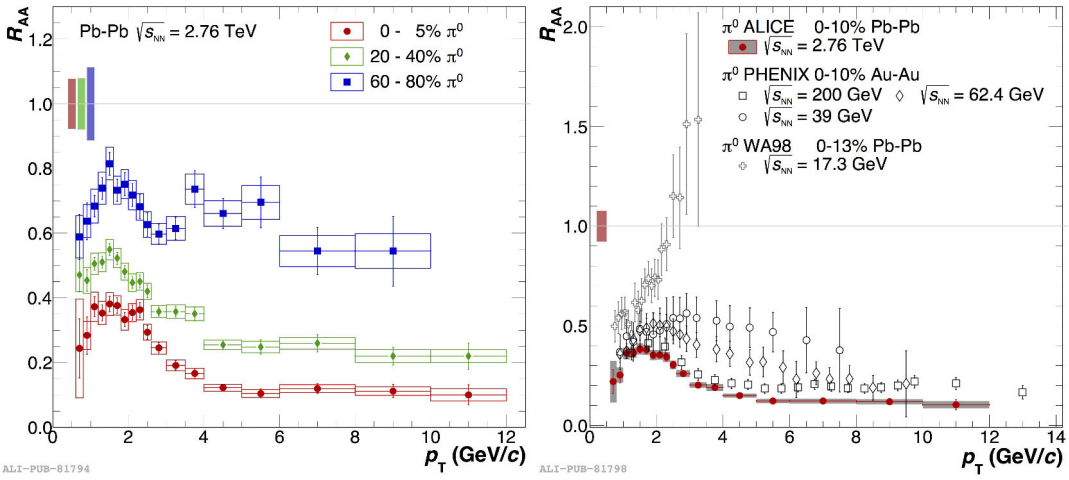

Figure 7. π^0 R_{AA} in three centrality classes in Pb−Pb collisions at $\sqrt{s_{\rm NN}}$ = 2.76 TeV (left panel) and comparison to previous experiments at lower centre-of-mass energies [10] (right panel).

20 GeV/c, and the measurement of η. In Fig. 8, the combined measurement from EMCal and PCM for two centrality classes is given for π^0 and η (left and right panel, respectively). The differential invariant yields are compared to the NLO pQCD predictions (with MSTW PDF and DSS14 (π^0), DSS07 (η) FF) scaled by N_{coll}, confirming the suppression of the neutral mesons yields in the Pb−Pb data.

In Fig. 9, the η/π^0 ratio is compared to the corresponding measurement in pp collisions at $\sqrt{s}$ = 7 TeV (left panel), to the pQCD predictions (middle panel, [2]) and to the ratio $K^{\pm}/\pi^{\pm}$ at the same centre-of-mass energy (right panel, [14]). A similar magnitude for the ratio is observed in both pp and Pb−Pb collisions, consistent with pQCD within the current experimental uncertainties [11]. The agreement of the η/π^0 ratio with the ratio $K^{\pm}/\pi^{\pm}$ implies no visible effects due to the strange quark content of the η and $K^{\pm}$ mesons.

6 π^0 and η spectra in p−Pb collisions at $\sqrt{s_{\rm NN}}$ = 5.02 TeV

Parton energy loss depends on the transport properties of the medium and their space-time evolution, the initial parton energy, and the parton type [10]. The nuclear modification factor, R_{AA}, is also affected by the slope of the initial parton transverse momentum spectrum prior to any interaction with the medium and initial-state effects like the modifications of the parton distributions in nuclei. An important constraint for modelling these effects comes from the study of p-A collisions [15].

ALICE has measured the neutral mesons differential invariant yields in p−Pb collisions at $\sqrt{s_{\rm NN}}$ = 5.02 TeV presented in Fig. 10 (left panel), fitted by a Tsallis function. The π^0 spectrum is the combined measurement from PCM, Dalitz, PHOS and EMCal, and the η spectrum from PCM and EMCal. The η/π^0 ratio is calculated and compared to the result from pp collisions at $\sqrt{s}$ = 7 TeV in Fig. 10 (right, up panel). As in the case of Pb−Pb data, the η/π^0 ratio in p−Pb collisions agrees with that obtained from pp collisions within the systematic and statistical uncertainties. The calculated π^0 R_{p-Pb} is consistent with unity above $p_T \gtrapprox 2.5$ GeV/c as shown in Fig. 10 (right, bottom panel). This measurement indicates that the strong suppression of hadron production at high p_T observed in Pb−Pb

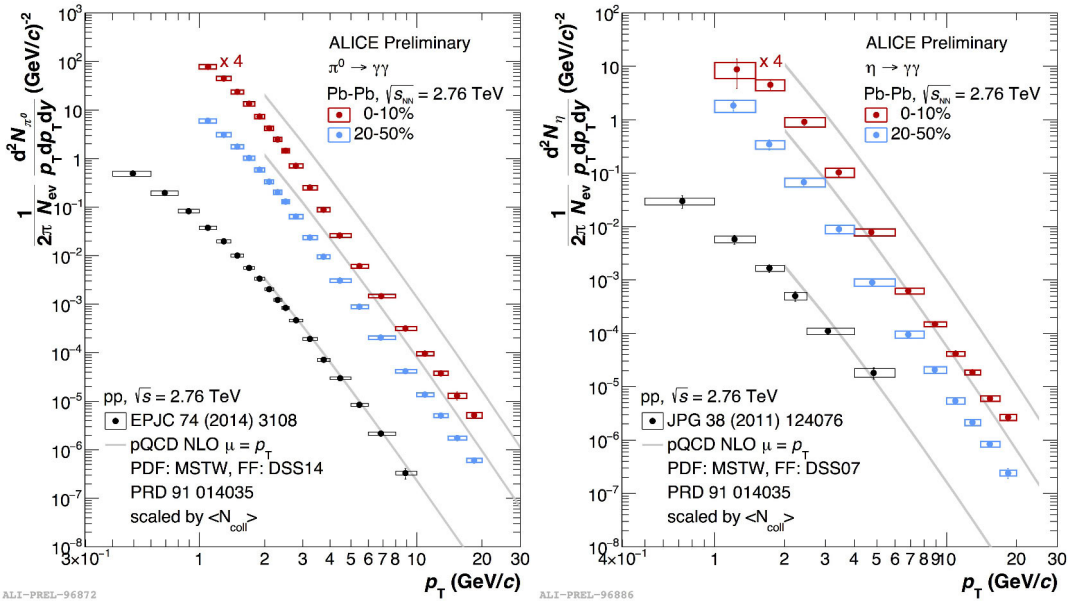

Figure 8. Combined invariant yield from EMCal and PCM in Pb−Pb collisions at $\sqrt{s_{\rm NN}}$ = 2.76 TeV compared to the pp reference at the same centre-of-mass energy for π^0 (left) and η mesons (right). The grey curves correspond to NLO pQCD calculations scaled by N_{coll}.

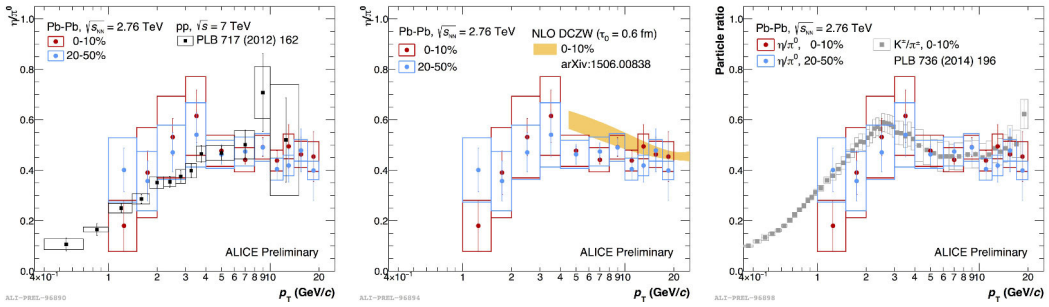

Figure 9. η/π^0 ratio in Pb−Pb collisions at $\sqrt{s_{\rm NN}}$ = 2.76 TeV and in two centrality classes compared to η/π^0 ratio in pp collisions at $\sqrt{s}$ = 7 TeV (left), to NLO pQCD predictions (middle) and to the $K^{\pm}/\pi^{\pm}$ in Pb−Pb collisions at $\sqrt{s_{\rm NN}}$ = 2.76 TeV (right).

collisions is not due to an initial-state effect, but is the fingerprint of jet quenching in hot QCD matter. The experimental result is also consistent with model calculations such as EPS calculations assuming three different fragmentation functions [16] and the Color Glass Condensate model [1].

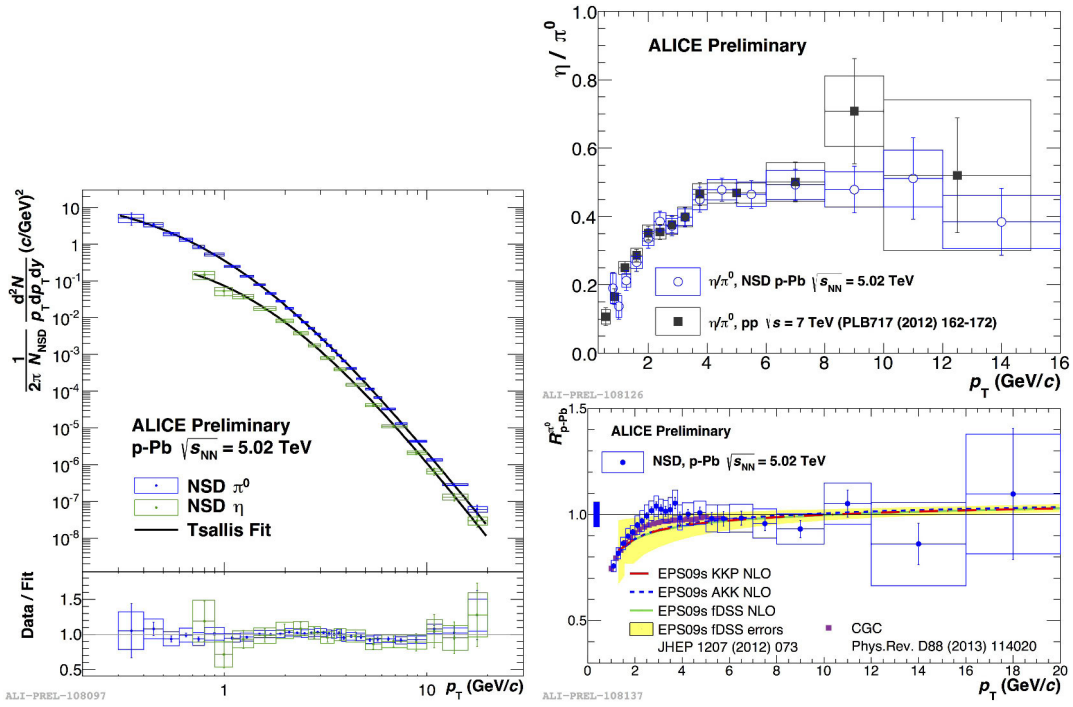

Figure 10. Left panel: π^0 and η spectra in p−Pb collisions at $\sqrt{s_{\rm NN}}$ = 5.02 TeV. Right, upper panel: η/π^0 ratio in p−Pb collisions at $\sqrt{s_{\rm NN}}$ = 5.02 TeV compared to η/π^0 ratio in pp collisions at $\sqrt{s}$ = 7 TeV. Right, bottom panel: π^0 R_{p-Pb} compared to model predictions.

7 Conclusions

The π^0 and η invariant cross sections are measured in pp, Pb−Pb and p−Pb collisions over a wide p_T range by using different and complementary detection methods. The pp results are compatible with NLO pQCD calculations at the lower p_T and collision energies, however, there is a growing discrepancy with increasing p_T and $\sqrt{s}$.

In Pb−Pb collisions, the π^0 invariant yields in different centrality classes and the measured R_{AA} show an increasing suppression with increasing centrality and centre-of-mass energy. The shape of R_{AA} is comparable between RHIC and LHC energies. However, at the LHC energies there is a stronger suppression observed resulting from the higher initial energy densities.

ALICE has also measured the π^0 and η invariant cross sections in p−Pb collisions to disentangle initial state effects from parton energy loss in the medium. Indeed, the R_{p-Pb} is found to be consistent with unity above $p_T \gtrapprox 2.5$ GeV/c, demonstrating that the strong suppression observed in central Pb−Pb collisions at the LHC is not due to an initial-state effect.

The η/π^0 ratio in the three systems, pp, Pb−Pb and p−Pb is consistent within the current statistical and systematic uncertainties and reaches a constant value for $p_T > 4$ GeV/c.

References

[1] T. Lappi, H. Mäntysaari, Phys. Rev. D **88**, 114020 (2013)

[2] W. Dai, X.F. Chen, B.W. Zhang, E. Wang, Phys. Lett. B **750**, 390 – 395 (2015)
[3] X. Guo, X. N. Wang, Phys. Rev. Lett. **85**, 3591 (2000)
[4] K. Aamodt et al., JINST **3**, S08002 (2008)
[5] ALICE Collaboration, Technical design report go the Photon Spectrometer, CERN/LHCC99-4
[6] ALICE Collaboration, Technical design report of the ALICE Electromagnetic Calorimeter, CERN/LHCC-2008-014 (2008)
[7] K. Aamodt et al., JINST **5**, P03003 (2010)
[8] J. Alme et al., Nucl. Instrum. Meth. A **622**, 316 – 367 (2010)
[9] B. Abelev, et al., Phys. Lett. B **717**, 162 – 172 (2012)
[10] B. Abelev et al., Eur. Phys. J. C **74**, 3108 (2014)
[11] A. Morreale et al., Nucl. Phys. A **00**, 1 – 4 (2015)
[12] D. de Florian, R. Sassot, M. Epele, R. J. Hernandez-Pinto, M., Stratmann, Phys. Rev. D **91**, 014035 (2015)
[13] C. A. Aidala, F. Ellinghaus, R. Sassot, J. P. Seele, M. Stratmann, Phys. Rev. D **83**, 034002 (2011)
[14] B. Abelev et al., Phys. Lett. B **736**, 196 – 207 (2014)
[15] B. Abelev et al., Phys. Rev. Lett. **110**, 082302 (2013)
[16] I. Helenius, K. J. Eskola, H. Honkanen and C. A. Salgado, JHEP, **073**, 1207 (2012)